CC BY

Exploring the Antioxidant and Antifungal Potential of *Couroupita guianensis Aubl* through *in Vitro* Assays, Molecular Docking, and Molecular Dynamics Simulations

Sujatha Jagannatha[1], Pavithra Bhavani Elango[1], Gouthami Kuruvalli[1], Challaraj Emmanuel ES[3], Vaddi Damodara Reddy[2], Ramanjaneyulu Golla[1*]

[1]Department of Biochemistry School of Allied Health Sciences, REVA University, Bangalore -560064, KA, India.
[2]Department of Biotechnology, School of Applied Sciences, REVA University, Bangalore -560064, KA, India.
[3]Department of Life Sciences, School of Biological & Forensic Sciences, Kristu Jayanti Deemed to be University, Bengaluru, Karnataka 560077, India.

Corresponding author: *Dr. Ramanjaneyulu G, Dept of Biochemistry, School of Allied Health Sciences, Email:ramanjaneyulu.golla@reva.edu.in , REVA University, Bangalore - 560064, Karnataka, India*

Abstract
Couroupita guianensis Aubl (cannonball tree) is a tropical plant known for its diverse bioactive constituents. The study evaluated the screening of phytochemicals, antifungal activity, and antioxidant potential of C. guianensis fruit extracts using experimental and in silico approaches. Fruit extracts were prepared using ethanol, methanol, ethyl acetate, and water. Phytoconstituents were identified by GC - MS. The scavenging activity of antioxidant was assessed using ABTS+ and DPPH+ radical-scavenging assays. Antifungal activity was evaluated against selected fungal strains, while molecular docking was used to examine interactions between identified compounds and fungal target proteins. The most promising complex was further investigated using molecular dynamics (MD) simulation. The extracts contained several bioactive compounds and exhibited concentration-dependent DPPH and ABTS scavenging activity at 5 - 100 µg/mL. The extracts also showed notable antifungal activity. Docking analysis demonstrated favorable interactions with Aspergillus niger endoglucanase and CYP51B, with binding energies ranging from -9.7 to -7.5 and -11.8 to -9.4 kcal/mol, respectively. Oxalic acid bis(6-ethyloct-3-yl) ester showed the most favorable binding profile. MD simulation further supported the stability of its interaction with A. niger endoglucanase. C. guianensis fruit extracts demonstrate promising antioxidant and antifungal properties, highlighting their potential as a source of bioactive compounds for further therapeutic investigation.

Keywords: *Couroupita guianensis Aubl*., Extraction, Purification, Active ingredient, Medicinal properties.

1. Introduction
The period in which medicinal plants have been using for the manufacture of indigenous medicines ranges from (Januardi et al., 2026). In Ayurveda sastra these plants are used as therapeutics are ornaments as these are best against different types of diseases. The cannon ball tree (*C. Guianensis*) is a fast-growing evergreen tree belong to the *Lecythidaceae* family (Kumar et al., 2011). These trees are mainly distributed in the parts of Brazil, America, South Caribbean and India. It is assumed sacred in Hindu religion due to the reason that the blossom of the tree looks like hood of holy Naga serpent, who protects the Shiva Lingam (Sumathi and Anuradha, 2017). These trees can be grown up to the height of 25 meters with 3-meter-wide branch and having the dimension of about 3 meters (Murugan and Mohan, 2011). These trees can be grown up to the size of 15-20 cm length and 15 cm width of large brown color spherical or cannonball shape fruits; thus the tree is famous by the name of cannon ball tree. These are the large hard woody fruit having small seed inside (Raju et al., 2023).

The fruit contains approximately 200–300 seeds and propagates through both self- and cross-pollination, facilitated by pollinating agents such as bees and bats (H. et al., 2022). Phytochemical investigations have identified various bioactive constituents, including fatty acids, terpenoids, and steroids. The alcoholic fruit extract is particularly rich in saponins, which have been associated with potential anticancer and cholesterol-lowering properties. In addition, antioxidant compounds present in the fruit can scavenge reactive free radicals, thereby helping to protect cells against oxidative stress and its associated cellular damage. Bioactive compounds have been used as the chief agent for developing anti-cancer and anti-inflammatory activities. The fruit pulp demonstrates antiseptic effect on wounds and infected skin of the animals (Shantilal et al., 2018; Sheba and Anuradha, 2019; Teixeira et al., 2019).

The phytochemicals from *C. guianensis* are utilized as an antifungal treatment, especially effective against fungal infections, dermatophyte issues, and skin lesions. They are also active in addressing chronic myelocytic leukaemia (Sheba and

Anuradha, 2019). The research by Bafna et al. indicated that the extract of plant shows antioxidant properties (Teixeira et al., 2019). Previous studies have reported that isatin, a bioactive compound isolated from the flowers of *C. guianensis*, possesses notable anticancer activity, particularly against human promyelocytic leukemia (HL-60) cells (Teixeira et al., 2019). Isatin can serve as a protective agent to counteract cancer caused by free radicals, as well as act as a therapeutic agent to eliminate cancer cells (Bafna and Mishra, 2010). Previous investigations have indicated that the methanolic fruit extract of *C. guianensis* has good anti-microbial and anti-biofilm efficacy against *Pseudomonas aeruginosa* (Jagannatha et al., 2025). Furthermore, secondary metabolites have the ability to fight against free radicals, and they appear to have higher antioxidant activity. The various solvent extractions have revealed rich in higher flavonoid contents, along with phenols and alkaloids (Augusco et al., 2023). The present study, we examined the molecular docking and dynamics investigations also performed the antioxidant scavenging activity and antifungal activity for identified phytochemicals efficacy on selected target protein.

2. METHODOLOGY

2.1. Preparation of *C. guianensis* plant fruit extract:

The organic solvent chosen for extraction is methanol and it was used with a plant material ratio of 1:5. To maximize the recovery of bioactive constituents, the plant material was initially separated from the extracts using muslin cloth (Tena and Asuero, 2022). The obtained filtrates were then subjected to filtration through Whatman No. 1 filter paper to eliminate residual particulate material. Solvent removal was accomplished *via* rotary evaporation under diminished pressure at 40 °C to achieve complete desiccation, producing approximately 6.5 g of crude extract. The resulting dried extract was transferred to sterile, sealed glass vessels, appropriately designated with identifying labels, and maintained at 4°C pending subsequent analytical procedures.

2.2. Phytochemical Analysis

The methanolic extract was tested for the presence of various phytochemicals. Qualitative analysis carried out for steroids, saponins, tannins, flavonoids, glycosides, aminoacids, sugars, coumarins, terpenoids, phenols and quinines as defined previously (Dubale et al., 2023).

2.3. Gas Chromatography - Mass Spectrometry (GC - MS)

The phytochemical constituents of *Couroupita guianensis* fruit extract were characterized using GC - MS (Thermo Scientific TRACE 1310 GC coupled with a TSQ 8000 triple quadrupole MS). Chromatographic separation was carried out on a TG-SMS capillary column (30 m × 0.25 mm, 0.25 µm film thickness) (Gomathi et al., 2015). Extract sample of 1.0 µL was introduced via injection employing a 1:30 split ratio. Helium served as the carrier gas, maintained at a constant flow rate of 1.0 mL/min. The chromatographic oven was initially maintained at 40°C for 2 minutes, subsequently elevated to 280°C at a heating rate of 20°C/min, and held at this terminal temperature for an additional 10 minutes. Mass spectral data were collected utilizing full-scan acquisition mode across an m/z range spanning 50 to 600. The retention indices of the detected compounds were determined using a homologous series of reference compounds. Putative compound identification was achieved by comparing the acquired mass spectra and retention indices with entries in the NIST spectral library. Molecular weight, molecular formula, structural information, and compound names were also considered for identification. The chromatographic profile of the crude methanolic extract showed multiple distinct peaks, indicating the presence of diverse secondary metabolites.

2.4. Anti - oxidant activity

2.4.1 Free Radical Scavenging activity by $DPPH^+$ assay

The antioxidant capacity of *C. guianensis* fruit extract, specifically its capacity to scavenge free radicals, was evaluated employing a marginally adapted DPPH+ radical-scavenging assay (Kuruvalli et al., 2024). Ascorbic acid served as the reference standard and was prepared in methanol at concentrations ranging from 5 to 100 µg/mL (5, 10, 20, 50, and 100 µg/mL). In the assay procedure, 1 mL of a 0.25% $DPPH^+$ solution was combined with the extract at the designated concentrations. The resulting reaction mixtures underwent incubation at 37°C for a duration of 30 minutes, after which absorbance measurements were obtained at 515 nm utilizing a UV-Vis spectrophotometer. Throughout the present investigation, all experimental procedures were executed in triplicate. The percentage of DPPH+ radical-scavenging activity was subsequently determined using the following equation:

$$\% \text{ Scavenging} = [(A_0 - A_1) / A_0] \times 100$$

In the equation, A_0 refers to the absorbance of the control, while A_1 represents the absorbance recorded for either the extract or the standard antioxidant, ascorbic acid.

2.4.2. Determination of ABTS Radical Cation Decolorization Activity

The free radical $ABTS^+$ scavenging assay relies on the light absorption properties of $ABTS^+$ radicals, and it was performed following established protocols outlined in previous literature (Hussen and Endalew, 2023). Since an antioxidant could potentially donate a hydrogen atom, a stable free radical can be quenched, and the difference in absorption could be detected with a spectrometer. The fairly stable radical $ABTS^+$ in a coloured green, can be observed on the spectrophotometer at 734 nm. The antioxidant capacity of the *C. guianensis* fruit extract was assessed through the $ABTS^+$ radical cation scavenging

assay methodology. $ABTS^+$ radical species were generated by combining equivalent volumes of ABTS and ammonium persulfate (APS) solutions, followed by incubation in darkness at ambient temperature for a duration of 14 -16 hours. The resulting radical solution employed for analytical examination was prepared by diluting the methanol solution (1:60 ratio) to attain an absorbance value proximate to 1.0 at a wavelength of 734 nm. In this assay, the $ABTS^+$ working solution was mixed with various concentrations of both the test extract and reference standard were prepared to achieve a total reaction volume of 1 mL. Absorbance measurements were obtained immediately at a wavelength of 734 nm utilizing a UV-Vis spectrophotometer. The percentage of radical inhibition was subsequently calculated for each concentration, and IC_{50} values were obtained using GraphPad Prism software. Radical-scavenging activity was determined using the following equation:

$$\% \text{ Inhibition} = \frac{(\text{Absorbance of Control} - \text{Absorbance of Sample})}{(\text{OD of Control})} \times 100$$

2.4. Antifungal activity

The in vitro antifungal efficacy of phytochemicals was evaluated against *Aspergillus niger*, *Penicillium sp.,* and *Fusarium sp*. through quantification of the inhibition zone concentration (ZIC). The compounds were applied at concentrations between 30 µg/ml and 90 µg/ml on Rose Bengal Agar to assess their antifungal activity. Following the streaking of fungi on each plate, they were allowed to incubate for 72 hours at 27°C. Each trial was conducted three times, and the ZIC was determined as the minimum concentration where macroscopic observation against a black backdrop indicated inhibition. Fluconazole served as the positive control, and DMSO was used as the blank control (Da et al., 2019).

2.5. Computational study

2.5.1 Selection of phytochemicals from *C. guianensis* for inhibitory design

Based on the GC - MS profiling results, seven identified phytochemicals were selected for further computational analysis. The respective 3D structural information was taken in SDF format from the PubChem database. The retrieved structures were converted into MOL format using ChemSketch and subsequently exported to PDB format using PyMOL for subsequent molecular modelling and structural analysis. The structure of Fluconazole was processed in a manner comparable to that of the reference control (Gouthami et al., 2022).

2.5.2 Drug likeliness prediction of phytochemicals

The drug-likeness of the selected phytochemicals was evaluated using the Molinspiration Cheminformatics platform. The analysis was performed according to Lipinski's Rule of Five, which is widely used to assess physicochemical properties associated with oral drug suitability. According to this rule, a compound generally exhibits favorable drug-like characteristics when its molecular weight is below 500 g/mol also, the number of hydrogen bond acceptors does not exceed 10, and the number of hydrogen bond donors is fewer than 5. Hydrogen bond donors and acceptors present in the structure of a drug are important for drug interactions with proteins, distribution, membrane permeability and water solubility (Prabhakaran et al., 2023).

2.5.3 ADMET properties

The ADMET profiles of the selected phytochemicals were predicted using the admetSAR online platform. The analysis was used to assess key pharmacokinetic and toxicity-related properties, including intestinal absorption, cytochrome P450 3A4 interactions, estrogen and androgen receptor activity, aromatase interaction, glucocorticoid receptor binding, OATP1B1 inhibition, UGT enzyme interactions, respiratory toxicity, reproductive toxicity, and aquatic toxicity. Based on the predicted ADMET characteristics, compounds exhibiting favorable pharmacokinetic profiles and lower toxicity risks were prioritized for further *in silico* evaluation through molecular docking studies (Gu et al., 2024).

2.5.4. Determination of protein targets and the creation of homology models

The selected protein sequences, including those identified through BLAST searches against the NCBI database, were subjected to structural and functional analysis using the CASTp server. Homology-based information was evaluated using sequence similarity searches, including BLAST and HHblits approaches. The analysis provided key parameters such as protein sequence length, sequence identity, alignment coverage, accession number, and total alignment score, which were considered for the selection and characterization of the target proteins. Active site residues of the protein were estimated by calculation server CastP as reported (http://sts.bioe.uic.edu/castp/calculation.html). The information of the active sites was obtained by considering 3 D structure and its surface area and volume data (Kumari et al., 2024).

2.5.5. Preparation of macromolecules

The macromolecules chosen for the docking studies are *Aspergillus niger endoglucanase* and PDB id: 1KS5 (Resolution: 2.10 Å), CYP51B PDB id: 4UYM (Resolution: 2.55 Å). The primary source of industrial cellulase is the fungus *Aspergillus niger*. Beta-1,4-Endoglucanase represents the main component of cellulase derived from *A. niger*. The enzyme CYP51B, also known as 14-α sterol demethylase, plays a key role in the biological process of sterol synthesis and is a main focus of antifungal drugs. By using of the Biovia Discovery Studio's visualizer tool, the large biomolecules were converted to PDB format, and three-dimensional studies on structure docking were executed (Gouthami et al., 2022)

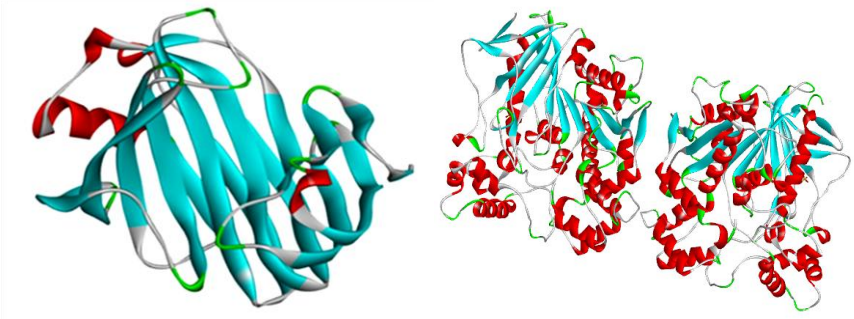


Fig. (1). Homology model of Aspergillus niger endoglucanase and CYP51B (1KS5, 4UYM)

The software AutoDock Vina 4.2 was employed for research on molecular docking to forecast the interactions between protein targets and their binding partners. The program evaluates the strength of the binding and the length of the bonds in the interactions between proteins and their binding associates.

2.5. Molecular Dynamics

The selected protein - ligand complexes were evaluated by 10 ns molecular dynamics simulations using the Schrödinger suite (Schrödinger LLC, New York, NY, USA). The complexes were prepared with the OPLS_2005 force field and solvated in a TIP3P water environment with a 10 Å buffer around the system. Molecular dynamics simulations were conducted at a temperature of 300 K and atmospheric pressure of 1 atm, employing a temporal integration step of 2 femtoseconds in conjunction with periodic boundary conditions. The Particle Mesh Ewald (PME) methodology was implemented to address long-range electrostatic interactions, while the SHAKE algorithm was applied to constrain covalent bonds involving hydrogen atoms. The structural stability and conformational dynamics of protein-ligand complexes were assessed through root-mean-square deviation (RMSD), root-mean-square fluctuation (RMSF), radius of gyration calculations, and hydrogen-bonding pattern analysis. Additionally, the binding free energy of the complexes was calculated utilizing the Prime MM-GBSA computational technique (Pulakuntla et al., 2024).

3. Experimental results and discussion

3.1. Qualitative analysis of phytochemicals of C. guianensis plant fruit extracts

Phytochemical screening of fruit extract by different solvent revealed the presence of different primary and secondary metabolites. Flavonoids, tannins, phenols and alkaloids are present as the major active components while saponins, carbohydrates and proteins are present in a moderate rate in different types of solvent extractions. **Table 1** shows the presence of various metabolites by using different solvent solution (Hayat et al., 2020).

Table 1. Phytochemicals screening by different solvents

Sample part	**Fruit extract**			
Extraction solvent	**Ethanol extract**	**Water extract**	**Ethyl extract**	**Methanol extract**
Flavonoids	+++	+++	++	+++
Phenols	+++	+++	++	+++
Tannins	+++	+++	+++	+++
Alkaloids	+++	+++	+++	+++
Saponins	+	++	+	+
Carbohydrate	+	+++	+	++
Steroids	++	Absent	++	+
Terpenoids	+	Absent	+	+
Proteins	++	++	+	++
Glycosides	+	Absent	++	+

Mild ; “++” = Medium; “+++” = Prominent

3.2. GC - MS analysis

GC-MS analysis confirmed that the phytochemical compounds are 9,19-Cyclolanost-24-en-3-ol acetate (3.beta.)-, 9,19-Cycloergost-24(28)-en-3-ol 4,14-dimethyl acetate(3.beta.,4.alpha.,5.alpha.)-, Clionasterol acetate, (3S,8S,9S,10R,13R,14S,17R)-17-((2R,5R)-5-Ethyl-6-methylheptan-2-yl)-3-methoxy-10,13-dimethyl 2,3,4,7,8,9,10,11,12,13,14,15,16,17-tetradecahydro-, 9,19-Cyclolanost-24-en-3-ol (3.beta.)-, Stigmasta-3,5-diene & Oxalic acid bis (6-ethyloct-3-yl) ester. Present in the C. Guianensis, and these compounds were used for further analysis (**Figs.2,3 & Table.2**).

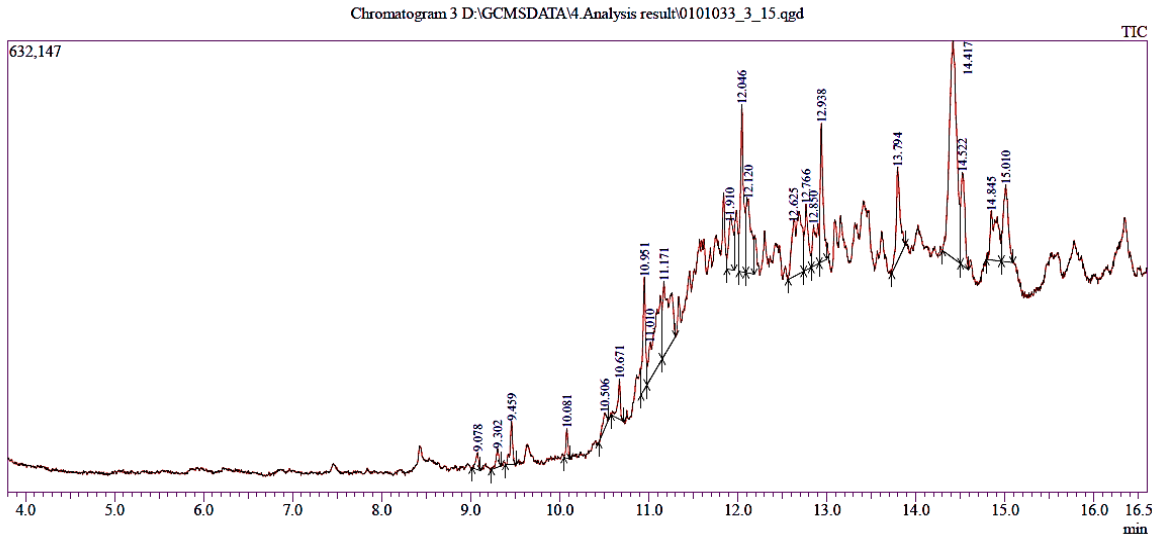


Fig. (2). GC-MS analysis *of C. guianensis* fruit extract

Table.2. List of compounds from GC-MS analysis

Peak	R. Time	Area	Area%	Height	Height%	A/H	Name
1	9.078	52925	0.65	23862	1.13	2.22	Dodecane, 2,6,11-trimethyl-
2	9.302	57278	0.70	25991	1.23	2.20	1-Octanol, 2-butyl-
3	9.459	119357	1.47	60983	2.89	1.96	Dodecane, 2,6,11-trimethyl-
4	10.081	60813	0.75	41165	1.95	1.48	Tetradecane
5	10.506	69379	0.85	21847	1.03	3.18	9,19-Cyclolanost-24-en-3-ol, acetate, (3.beta.)-
6	10.671	110776	1.36	56197	2.66	1.97	9,19-Cycloergost-24(28)-en-3-ol, 4,14-dimethyl,acetate,(3.beta.,4.alpha.,5.alpha.)-
7	10.951	319296	3.92	157276	7.45	2.03	Clionasterol acetate
8	11.010	622725	7.65	52518	2.49	11.86	(3S,8S,9S,10R,13R,14S,17R)-17-((2R,5R)-5-Ethyl-6-methylheptan-2-yl)-3-methoxy-10,13-dimethyl-2,3,4,7,8,9,10,11,12,13,14,15,16,17-tetradecahydro-
9	11.171	565343	6.95	104758	4.96	5.40	9,19-Cyclolanost-24-en-3-ol, (3.beta.)-
10	12.046	567027	6.97	234386	11.10	2.42	Stigmasta-3,5-diene
11	12.120	417978	5.14	103716	4.91	4.03	Oxalic acid, bis(6-ethyloct-3-yl) ester
12	12.625	621912	7.64	76164	3.61	8.17	Nerolidol 1
13	12.766	256195	3.15	92479	4.38	2.77	Hexadecane
14	12.850	236563	2.91	57485	2.72	4.12	Hexadecanoic acid, methyl ester
15	12.938	438441	5.39	194338	9.20	2.26	Eicosane
16	13.794	401155	4.93	131772	6.24	3.04	Octacosane
17	14.417	1761692	21.65	304228	14.41	5.79	beta.-Sitosterol acetate

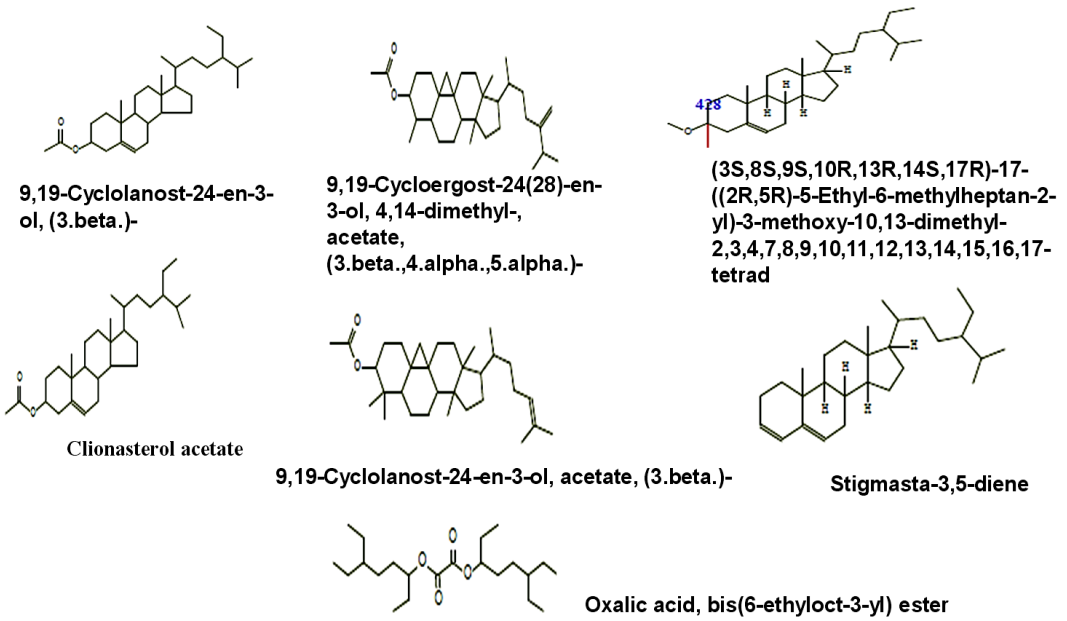


Fig. (3). Structures of compounds from GC-MS analysis of *C. guianensis* fruit extract

3.3. DPPH$^+$ and ABTS$^+$ radical scavenging activity

Preliminary phytochemical analysis of the methanolic *C. guianensis* fruit extract exhibited the presence of terpenoids, saponins, alkaloids, glycosides, and reducing sugars. The extract was also found to contain measurable amounts of phenolic compounds, flavonoids, and tannins (**Fig. 4**). Both ABTS$^+$ and DPPH$^+$ scavenging activities significantly increased with increasing extract concentration from 5 to 100 µg/mL, as illustrated in **Fig. 4a and 4b** (Munteanu and Apetrei, 2021). The calculated IC_{50} values were 49.9 µg/mL for DPPH$^+$ and 47.2 µg/mL for ABTS$^+$. Ascorbic acid and gallic acid served as standard antioxidants for comparison.

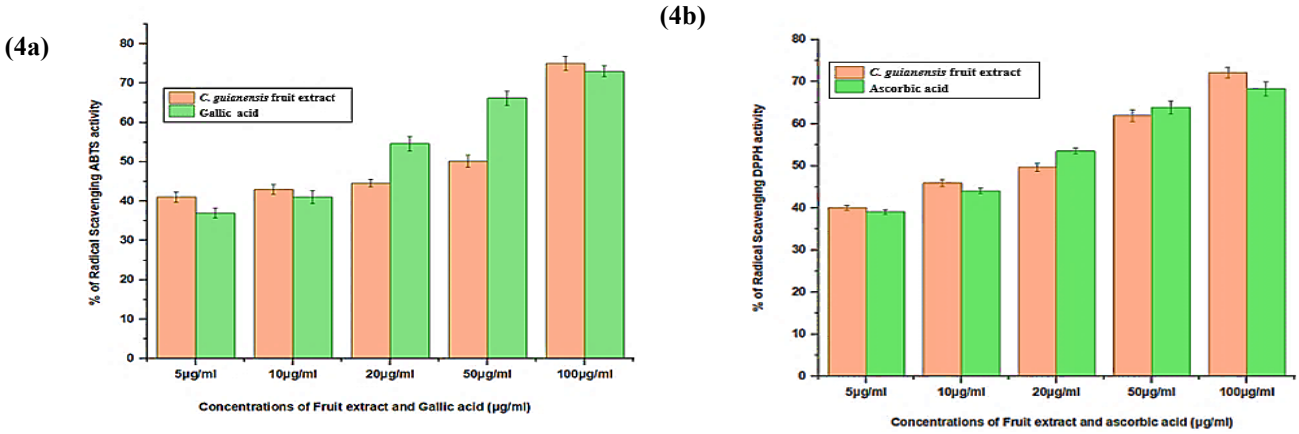


Fig. (4). 4a and 4b illustrate the radical-scavenging efficacy of *C. guianensis* fruit extract against DPPH+ and ABTS$^+$ radicals. The presented values denote the mean ± standard deviation derived from three independent experimental replicates conducted according to the procedures outlined in the methodology section. Statistical significance was established at a threshold of $p < 0.05$.

Table.3. Anti-fungal activity of *C. guianensis* fruit extract

Sl. No	Concentration of the sample	*Aspergillus niger*	*Fusarium sp.*	*Penicillium sp.*
1	30µg/ml	6.01±0.32	6.01±0.31	6.02±0.32
2	40µg/ml	6.03±0.33	6.04±0.31	6.03±0.31
3	50µg/ml	6.06±0.31	6.06±0.31	6.04±0.31
4	60µg/ml	6.12±0.32	6.14±0.33	6.13±0.33
5	70µg/ml	6.23±0.31	6.19±0.32	7.3±0.31
6	80µg/ml	8.1±1.32	6.22±0.31	9.43±1.67
7	90µg/ml	9.2±1.96	6.24±0.32	11.8±2.87
8	Fluconazole (+ Control)	12.1±2.34	12.8±2.97	13.7±3.28
9	DMSO (- Control)	6±0.32	6±0.31	6±0.33

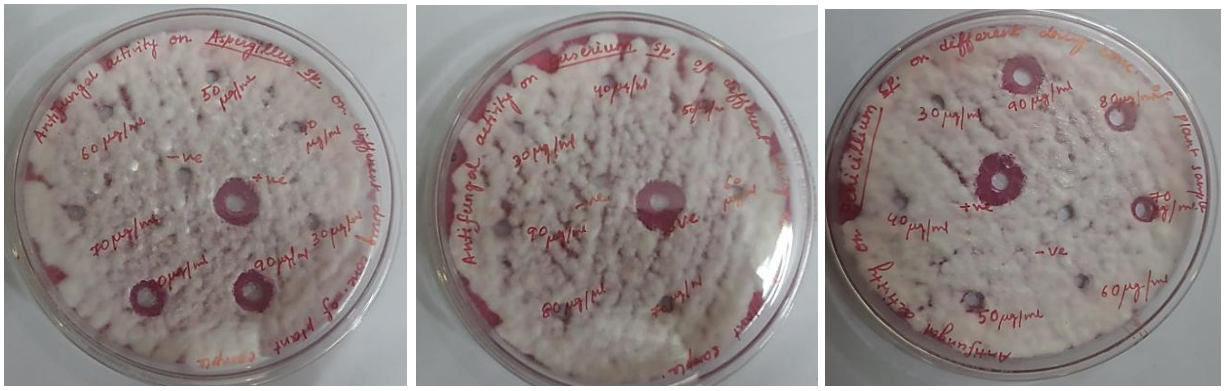


Fig. (5). Anti-fungal activity of *C. guianensis* fruit extract and Fluconazole

3.4. Molecular Docking

3.4.1. AMDET analysis of compounds

Key molecular descriptors, including molecular weight, AlogP, rotatable bond count, and the numbers of hydrogen-bond donors and acceptors, are important determinants of drug-like properties. These parameters are commonly assessed according to Lipinski's rule of five, can provides an initial identification of a compound's distribution, absorption, metabolism, and excretion (ADME) characteristics. To evaluate the drug-like properties of synthetic molecules, reference drugs can be utilized and represented in (**Table.4**) (Lipinski, 2004).

Table.4. Pharmacophore analysis of *C. guianensis* fruit extract phytochemicals with reference drug

Sl.No	Compounds	Molecular weight (g/mol)	Alo g P	H-Bond acceptor	H-Bond donor	Rotatable bond
1	9,19-Cyclolanost-24-en-3-ol, acetate, (3.beta.)-	456.75	2	0	1	8
2	9,19-Cycloergost-24(28)-en-3-ol, 4,14-dimethyl,acetate,(3.beta.,4.alpha.,5.alpha.)-	468.77	2	0	1	7
3	Clionasterol acetate	498.88	1	0	1	7
4	(3S,8S,9S,10R,13R,14S,17R)-17-((2R,5R)-5-Ethyl-6-methylheptan-2-yl)-3-methoxy-10,13-dimethyl-2,3,4,7,8,9,10,11,12,13,14,15,16,17-tetradecahydro-	456.75	2	0	1	8
5	9,19-Cyclolanost-24-en-3-ol, (3.beta.)-	468.77	2	0	1	6
7	Stigmasta-3,5-diene	452.81	0	0	1	6
8	Oxalic acid, bis(6-ethyloct-3-yl) ester	370.57	4	0	1	17
9	Fluconazole	306.28	0.74	7	1	5

3.5.2. In silico Bioactivity study

The Molinspiration Cheminformatics server was used to evaluate the biological activity scores of the synthetic compounds. Gaining insight into the active sites or binding mechanisms through these studies is crucial for understanding the biological behavior of the compounds represented in (**Table.5**) (Srivastava, 2021).

Table.5. Biological activity of phytochemicals with reference drug

Sl.no	Compounds	GPCR Ligand	Ion channel modulator	Kinase inhibitor	Nuclear receptor ligand	Protease inhibitor	Enzyme inhibitor
1.	Ligand_1	12	0.02	-0.59	0.60	0.03	0.43
2.	Ligand_2	0.06	0.09	-0.43	0.76	0.02	0.53
3.	Ligand_3	0.29	0.10	-0.20	0.51	0.17	0.39
4.	Ligand_4	0.08	0.02	-0.59	0.60	0.03	0.43
5.	Ligand_5	0.11	0.07	-0.50	0.73	0.09	0.57
6.	Ligand_6	0.26	0.08	-0.17	0.64	0.07	0.44
7.	Ligand_7	0.07	0.02	-0.18	0.14	0.17	0.10
8.	Fluconazole	0.04	0.01	-0.09	-0.23	-0.09	0.03

ADMET characteristics, encompassing absorption, distribution, metabolism, excretion, and toxicity, are important considerations in the early stages of drug development. In addition to demonstrating activity against the intended therapeutic target, a potential drug candidate should exhibit acceptable pharmacokinetic behavior and safety at therapeutically relevant concentrations. Therefore, the selected compounds were further evaluated for drug-likeness and potential toxicity using the ADMETsar platform (Dulsat et al., 2023) (Table.6).

Table.6. ADME properties of phytochemicals with reference drug

S.no	compounds	GI absorption	BBB permeant	P-gp substrate	CYP1A2 inhibitor	CYP2C19 inhibitor	CYP2C9 inhibitor	CYP2D6 inhibitor	CYP3A4 inhibitor	Log K_p (skin permeation)
1.	Ligand_1	low	–	–	–	–	–	–	–	-8.76 cm/s
2.	Ligand_2	High	–	–	+	–	–	+	+	-7.05 cm/s
3.	Ligand_3	High	–	–	+	–	–	+	+	-6.70 cm/s
4.	Ligand_4	Low	–	+	–	–	–	–	–	-10.26 Cm/s
5.	Ligand_5	High	–	+	–	–	–	–	–	-7.82 cm/s
6.	Ligand_6	Low	–	+	–	–	–	–	–	-3.87 Cm/s
7.	Ligand_7	High	–	+	–	–	–	–	–	-7.82 cm/s
8.	Fluconazole	Low	–	+	–	–	–	–	–	-1.86 cm/s

No represent "–"
Yes represent "+"

3.5.3. Preparation of macromolecule and ligands for docking

Basic Local Alignment Search Tool (BLAST) is a normally utilized bioinformatics applications for discovering sequence similarities by comparing nucleotide or protein sequences with sequences accessible in biological databases. BLAST finds similarity between the query sequence and the database entries, assesses the statistical significance of the matches and allows fast alignments to be performed (**Table.7, Table. 8**) (Altemimi et al., 2017).

Table:7. Prediction of the Target Protein Active Site by CASTp Analysis

Sl.no	Selected protein name	PDB code	Total area (SA) Å^2	Total volume (SA) Å^3	Active residues
1.	*Aspergillus niger endoglucanase*	1KS5	376.826	286.819	Trp22, Val58, Tyr61, Asp95,Thr110, Ser112, Asp114, Glu116, Trp120, Gln128, Ile130, Gln153, Glu204.
2.	CYP51B	4UYM	7607.219	14787.926	Phe234, Tyr68, Lue91, Phe504, Ile373, Tyr122, Tyr136, Lys147, Val135 and Ala307.

Table:8. BLASTp-Based Identification of the Target Protein

Sl.no	Selected protein name	Sequence length	ID of sequence	Total % of identify	Total Sequence coverage	Total score
1.	*Aspergillus niger endoglucanase*	239	XP_035351835.1	100	16-239	486
		239	XP_025480224.1	100	1-239	484
		239	XP_025480224.1	100	1-239	483
2.	CYP51B	524	KAl2965992.1	92	52-518	881
		524	GKZ70193.1	90	52-518	881

For molecular docking analysis, the homology-modelled proteins were prepared by adding polar hydrogens and assigning Gasteiger partial charges. The selected phytochemicals and reference drugs were prepared by defining rotatable bonds and appropriately assigning hydrogen atoms. Docking calculations were performed using AutoDock Vina, with a grid box of 40 × 40 × 40 points centered at X = 90.917, Y = 87.491, and Z = 85.771 Å, with a spacing of 0.672 Å. The generated grid maps were used to explore ligand-binding poses within the active site. A configuration file containing the required docking parameters was prepared and submitted to AutoDock Vina to predict the binding modes and affinities of the selected ligands toward the target proteins (Cosconati et al., 2010).

Table.9. The docking score of *Aspergillus niger* endoglucanase against identified bioactive compounds with reference drug

Bioactive compounds with reference drug	Binding affinity (kcal/mol)	Interacting amino acids	Types of residue bonds	Bond distance (Å)
Ligand_1	-8.9	Asn20, Gln200 Trp22, Val58	H-bond Pi-Alkyl	3.04, 3.22 3.67, 4.20
Ligand_2	-9.9	Asn20, Gln200 Trp22 Trp120	H-bond Pi-Sigma Pi-Alkyl	3.05, 2.93 3.64 4.27
Ligand_3	-7.5	Ser111 Ile130, Met118	H-bond Pi-Alkyl	3.59 4.86, 5.14
Ligand_4	-8.2	Gln200, Asn20 Trp22, Ile130	H-bond Pi-Alkyl	3.25, 3.26 3.21, 4.16
Ligand_5	-9.1	Ser111 Trp22 Met118, Ile130	H-bond Pi-Sigma Pi-Alkyl	3.46 3.96 3.76, 4.37
Ligand_6	-7.6	Phe206, Val58, Ile130, Trp22	Pi-Alkyl	4.30, 4.45 4.96, 4.30
Ligand_7	-9.7	Gln200, Ser111, Asn20, Asn63 Tyr7 Tyr61	H-bond Pi-Alkyl Pi-Sigma	3.17, 3.12 3.13, 3.04 3.41 3.88
Fluconazole	-7.1	Gln200, Asn20, Thr116, Asn63	H-bond	2.92, 3.10, 2.53, 2.92

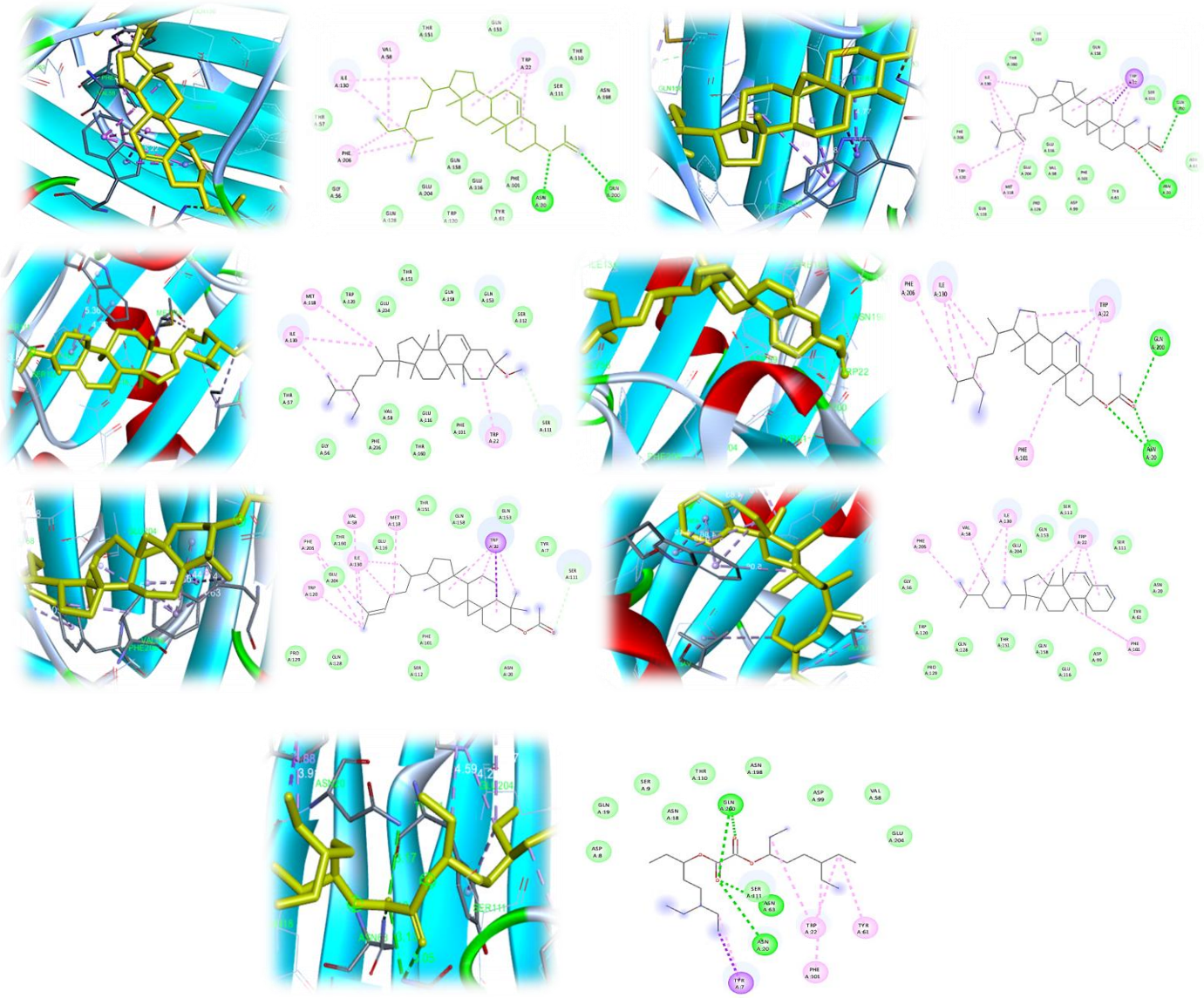


Fig. (6). Phytochemicals interaction of 2dimentional and 3dimentional interactions with *Aspergillus niger endoglucanase*.

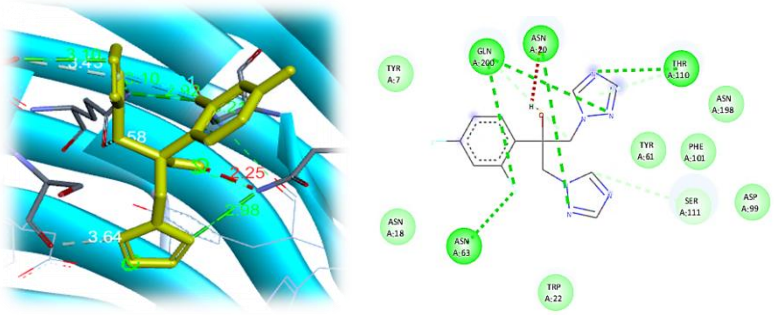


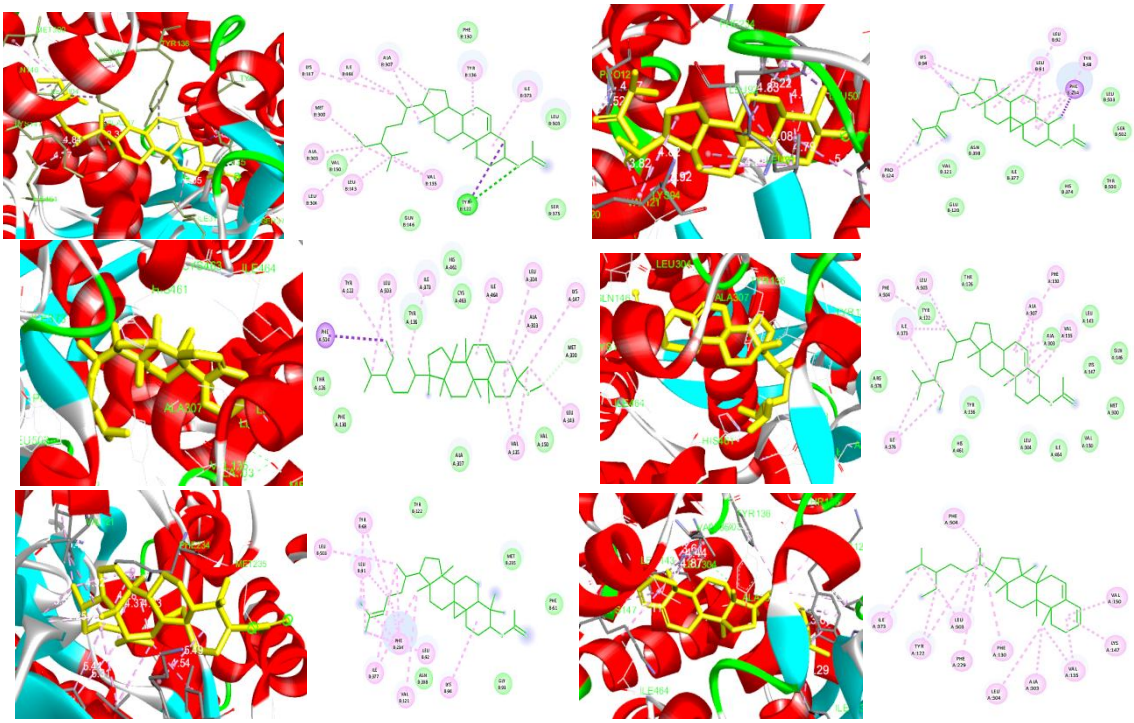
Fig. (7). Fluconazole 2dimentional and 3dimentional interactions with *Aspergillus niger endoglucanase*.

Molecular docking analysis indicated that several selected phytochemicals exhibited stronger predicted binding toward Aspergillus niger endoglucanase than the reference drug. Also, from the tested compounds, Ligand_2 shown the strong favorable docking score (-9.9 kcal/mol), forming H-bond interactions with Asn20 and Gln200, along with π-alkyl and π-sigma interactions involving Trp22, Trp120, and Tyr7. The corresponding interaction distances were 4.27, 2.93, 3.05, 3.64, and 2.70 Å, respectively. Ligand_7 exhibited a docking score of −9.7 kcal/mol and formed H - bonds with Gln200, Ser111, Asn20, and Asn63, together with a π-sigma interaction with Tyr7, with bond distances of 3.17, 3.12, 3.13, 3.04, and 3.41 Å, respectively (Fig. 6). Ligand_1 was identified as the third-ranked compound, along with a docking score of -8.9 kcal/mol. Also, can formed hydrogen bonds with Asn20 and Gln200 and π-alkyl interactions with Trp22 and Val58, with interaction distances of 3.04, 3.22, 3.67, and 4.20 Å, respectively (Fig. 6). In comparison, the reference drug fluconazole displayed a docking score of −7.1

kcal/mol and formed four H-bonds with Gln200, Asn20, Thr116, and Asn63, with distances of 2.92, 3.10, 2.53, and 2.92 Å, respectively (Fig. 7). Overall, the docking results suggest that Ligand_2, Ligand_7, and Ligand_1 may have favorable interactions with A. niger endoglucanase.

Table.10. The docking score of CYP51B against identified bioactive compounds with reference drug

Bioactive compounds with reference drug	Binding affinity (kcal/mol)	Interacting amino acids	Types of residue bonds	Bond distance (Å)
Ligand_1	-10.3	Tyr122 Met300, Leu143	H-bond 2 Pi-Alkyl	3.33 4.17, 4.23
Ligand_2	-10.8	Phe234 Tyr68, Lue91	Pi-Sigma 2 Pi-Alkyl	4.82 4.79, 4.22
Ligand_3	-12.2	Phe504 Ile373, Tyr122	Pi-Sigma 2 Pi-Alkyl	3.59 4.86, 5.14
Ligand_4	-9.6	Phe130, Leu503, Ile373	3 Pi-Alkyl	3.25, 3.26, 3.21
Ligand_5	-9.9	Val121, Lue92 Thr687	3 Pi-Alkyl	3.46, 3.96, 3.76
Ligand_6	-11.8	Phe504, Ile503 Ala303	3 Pi-Alkyl	4.30, 4.45, 4.96
Ligand_7	-9.4	Tyr136 Lys147, Val135, Ala307	H-bond 3 Pi-Alkyl	2.98 3.58, 4.73, 5.20
Fluconazole	-7.4	Tyr470, Leu471 Ala360	H-bond 2 Pi-Alkyl	3.12 4.10, 3.53



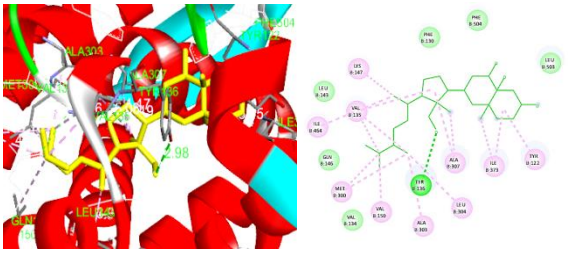


Fig. (8). Phytochemicals interaction of 2dimentional and 3dimentional interactions with CYP51B.

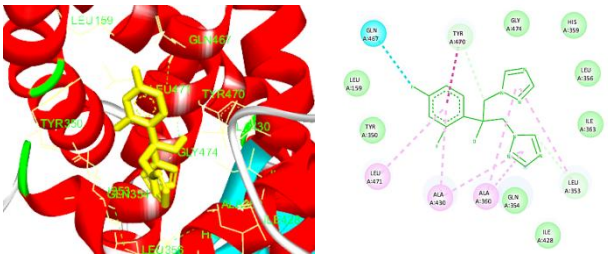


Fig. (9). Fluconazole 2dimentional and 3dimentional interactions with CYP51B.

The molecular docking analysis shown that the phytochemical compounds revealed stronger binding affinity toward CYP51B than the reference compound. The binding energies of the identified phytochemicals ranged from -11.8 to -9.4 kcal/mol. Among the screened compounds, Ligand_1 emerged as one of the most promising candidates, displaying a docking score of -10.3 kcal/mol. It formed a hydrogen bond with the amino acid residue Tyr122 and two π-alkyl interactions with Met300 and Leu143. The corresponding bond lengths were 3.33 Å, 4.17 Å, and 4.23 Å, respectively (Fig. 8). Ligand_7 shown a docking score of -9.4 kcal/mol and established one hydrogen bond with Tyr136, along with three π-alkyl interactions involving Lys147, Val135, and Ala307. The bond distances for these interactions were 2.98 Å, 3.58 Å, 4.73 Å, and 5.20 Å, respectively (Fig. 8). In comparison, the reference antifungal drug Fluconazole exhibited a docking score of -7.4 kcal/mol. It formed a hydrogen bond with Tyr470 and two π-alkyl interactions with Leu471 and Ala360. The corresponding bond lengths were 3.12 Å, 4.10 Å, and 3.53 Å, respectively (Fig. 9).

The docking results suggest that the phytochemicals identified from Couroupita guianensis fruit extract possess favorable interactions with CYP51B and exhibit stronger binding affinities than the reference drug. These findings support the potential antifungal activity of the extracted phytochemical constituents and highlight their suitability as promising candidates for further investigation.

3.5.4. Molecular Dynamics Simulations

All simulation results were analysed for the compound by using molecular dynamics (MD) simulation for 100 ns to understand the protein - ligand dynamics. RMSD, RMSF, protein -ligand contacts, 2D interaction profiles, and ligand properties were analysed to assess complex stability, flexibility, and interaction patterns during the simulation. In **Fig.10** the root mean square deviation plot of *Aspergillus niger* endoglucanase in complex with Oxalic acid bis (6-ethyloct-3-yl) ester (protein-ligand) shown. It can be observed that the entire protein–ligand complexes showed the possibility of binding as it remains below 2 Å (Ghahremanian et al., 2022)

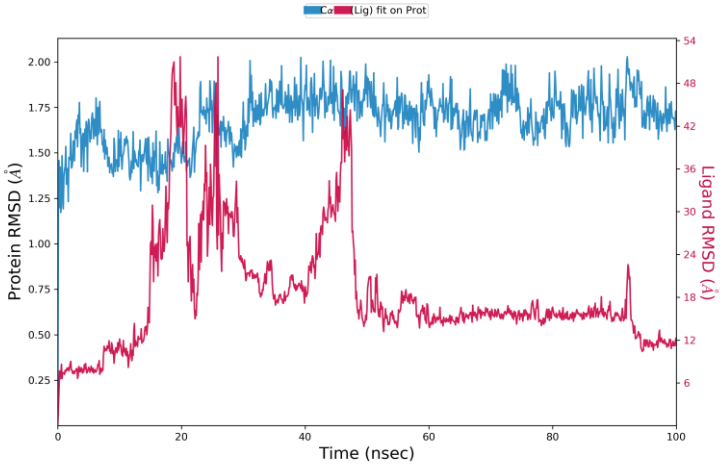


Fig. (10). RMSD plot of the protein- Oxalic acid bis (6-ethyloct-3-yl) ester complex.

Additionally, to investigate the changes of amino acids within the protein and those in direct contact with the protein, root mean square fluctuation (RMSF) plots were generated for the protein-ligand complex. The green vertical lines denote the amino acids that interact with the ligands. The RMSF plot corresponding to the protein-oxalic acid bis(6-ethyloct-3-yl) ester complex is presented in Figure 11. In the protein-oxalic acid bis(6-ethyloct-3-yl) ester complex, the deviations exhibited by amino acids that interact with the protein are notably smaller in magnitude compared to those of non-interacting residues. This is because the deviations are smaller for higher interaction between protein and ligands. The nature of interactions is further revealed by plotted ligand-protein map as depicted in Fig. 12 where the green and grey colours denote hydrogen and hydrophobic interaction, pink denotes ionic interaction and blue denote water bridges.

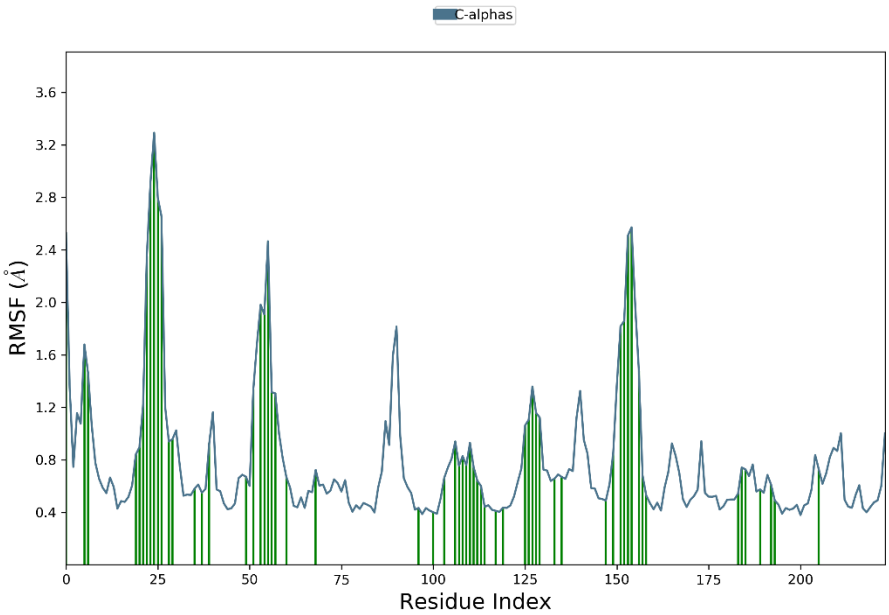


Fig. (11). RMSF plot of the protein- Oxalic acid bis (6-ethyloct-3-yl) ester complex.

During approximately 50% of the molecular dynamics simulation, TYR7 was involved in hydrophobic interactions with the ligand. In addition, GLY23 maintained a stable hydrogen bond with the ligand for nearly 70% of the simulation period. Significant interactions were also observed with TRP22, GLU55, and GLN128, indicating their important roles in stabilizing the protein–ligand complex. Furthermore, ALA154 and GLU157 interacted with Oxalic acid bis (6-ethyloct-3-yl) ester through a combination of water-mediated bridges, hydrophobic contacts, and hydrogen bonds. As a result, these amino acid residues exhibited persistent and multiple interactions throughout the simulation, contributing to the overall stability of the complex.

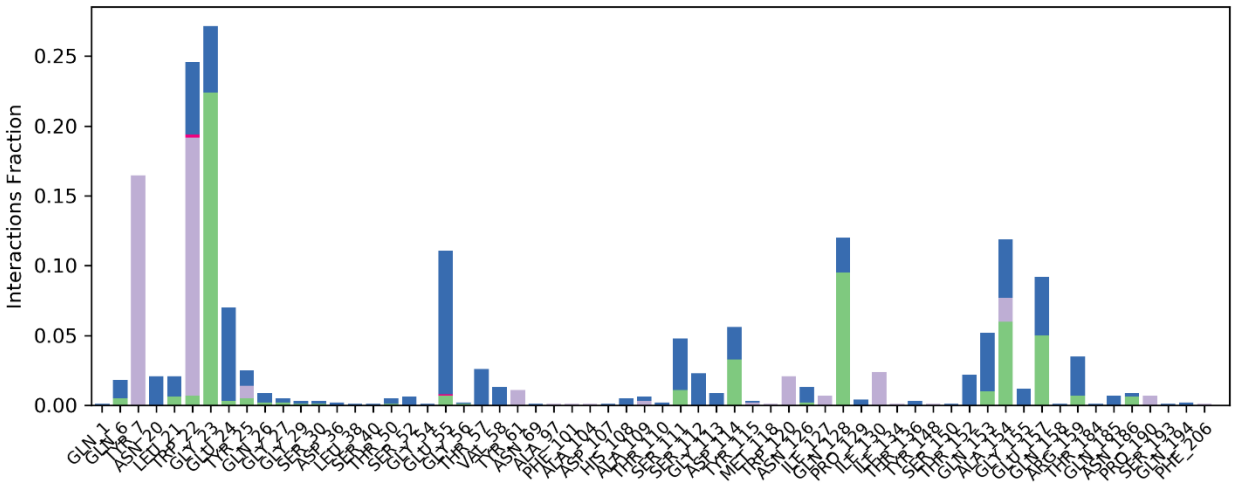


Fig. (12). Interaction Contact Map of the Protein Bound to Oxalic Acid bis(6-ethyloct-3-yl) Ester

The dynamic behavior and ligand-related properties of the Protein–Oxalic acid bis (6-ethyloct-3-yl) ester complex were evaluated during the molecular dynamics simulation, and the observed variations are illustrated in Fig. 13. Throughout the simulation, the analyzed ligand parameters remained relatively stable, indicating consistent ligand behavior within the binding pocket. The RMSD profile of the Protein–Oxalic acid bis (6-ethyloct-3-yl) ester complex exhibited only minor fluctuations,

with average RMSD values of 0.73 Å for the protein and 4.97 Å for the ligand, suggesting overall structural stability of the complex. Furthermore, the solvent-accessible surface area (SASA) and related solvent exposure properties of Oxalic acid bis (6-ethyloct-3-yl) ester showed average values of 144.08 Å² and 715.82 Å², respectively, reflecting the ligand's interaction with the surrounding solvent environment during the simulation (**Fig. 13).**

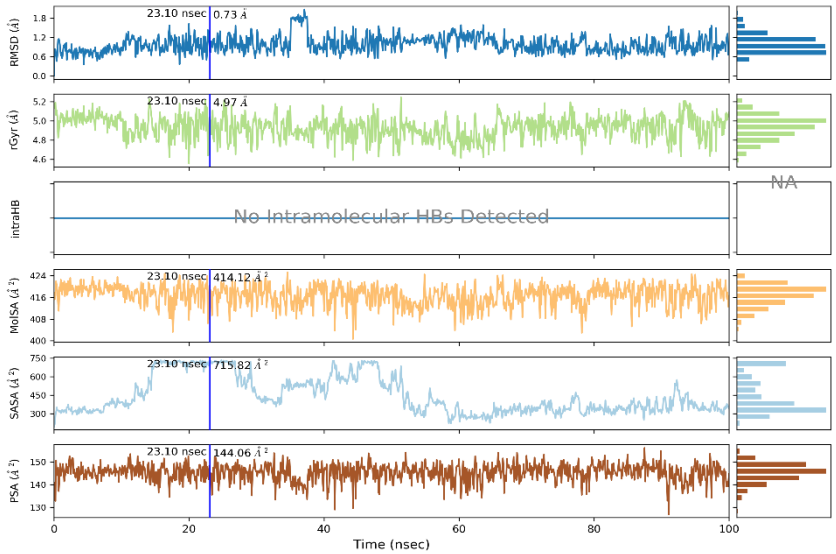


Fig. (13). The properties of the ligand in the protein- Oxalic acid bis (6-ethyloct-3-yl) ester complex evaluated during the simulation period of 100 ns.

The rotational characteristics of the torsional bond present in the Oxalic acid bis(6-ethyloct-3-yl) ester ligand are depicted through a radial plot and corresponding bar charts rendered in consistent coloration (Fig. 14). The torsional profile of the ligand documents the conformational variations occurring at each rotatable bond throughout the simulation trajectory, spanning the temporal range from 0 to 100 nanoseconds (Gheidari et al., 2024). The radial graphs show how the torsion varied throughout the simulation, with each line outward representing the temporal evolution starting from the middle (radius). The axis Y of the bar graphs represents the rotational bond potential in Kcal/mol. As well as the torsional potential, the overall potential produced by the rotations of all the rotatable bonds is represented. Radial graphs as well as bar graphs were used to compare how torsional potential correlates with the strain of structure in Oxalic acid bis (6-ethyloct-3-yl) ester ligand structure.

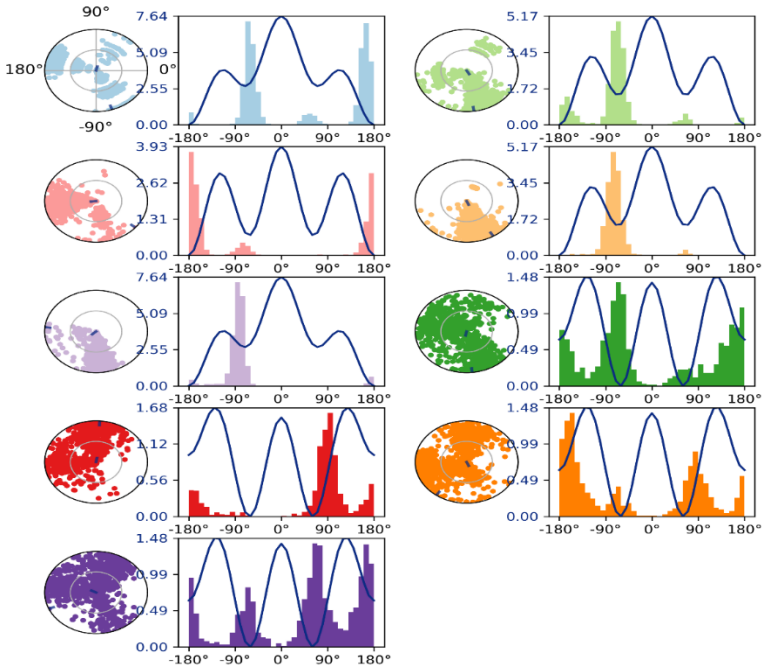


Fig. (14). Details of rotatable bonds during MD simulation

4. Conclusion

As the extracts from *Couroupita guianensis* have numerous effects on treating several diseases it could serve a great impact on society by replacing the conventional drugs used in world of medicines. For indeed explanation the regular drugs that are being used from a long period of time they show side effects on the body, but these extracts can use instead of the drugs. The extraction of metabolites from fruit using solvents like Methanol, Ethyl acetate, Ethanol and Water were purified to get major active medicinal ingredient by using column chromatography or selective solvent method. By gas chromatography-mass spectrometry (GC–MS) analysis different several phytochemicals identified. Phytochemical screening of the methanolic *C. guianensis* fruit extract reveals the existence of saponins, terpenoids, glycosides, alkaloids, and reducing sugars. The extract demonstrated concentration-dependent $DPPH^+$ and $ABTS^+$ radical-scavenging activity over the tested range of 5 -100 µg/mL, with IC_{50} values of 49.9 and 47.2 µg/mL, respectively. Ascorbic acid and gallic acid were used as reference standards. The extract also exhibited *in vitro* antifungal activity against *Aspergillus niger, Penicillium sp.,* and *Fusarium sp*. using the cup-plate agar diffusion method, with fluconazole and DMSO serving as controls. Molecular docking analysis indicated favorable interactions between the selected phytochemicals and the target proteins. Among the identified compounds, Oxalic acid bis(6-ethyloct-3-yl) ester showed promising binding toward A. niger endoglucanase. Subsequent molecular dynamics simulation demonstrated that the protein–ligand complex maintained stable interactions throughout the simulation period. These findings suggest that *C. guianensis* fruit contains bioactive constituents with antioxidant and antifungal potential and provides a basis for further investigation of the identified phytochemicals as potential antifungal leads against *A. niger*.

Ethical statement

Not applicable

Conflict of interest

The authors declare that they have no conflict of interest

Acknowledgements: Authors thanks REVA University for providing all necessary facilities to carry out research work.

References

1. Januardi, M.R., Setiawan, F., Islamie, R., Sukweenadhi, J., Wungsintaweekul, B., Kartini, K., 2026. Medicinal plants for hemorrhoid therapy: Mechanistic insights, bioactive compounds, and preclinical-to-clinical evidence. Journal of Applied Pharmaceutical Science, 16, pp.776–794.
2. Kumar, C.S., et al., 2011. A short review on therapeutic uses of Couroupita guianensis Aubl. International Research Journal of Pharmacy and Applied Sciences, 1, pp.105–108.
3. Sumathi, S., Anuradha, R., 2017. Couroupita guianensis Aubl: An updated review of its phytochemistry and pharmacology. Asian Journal of Pharmaceutical and Clinical Research, 3, pp.1–8.
4. Murugan, M., Mohan, V.R., 2011. Evaluation of phytochemical analysis and antibacterial activity of Bauhinia purpurea L. and Hiptage benghalensis L. Kurz. Journal of Applied Pharmaceutical Science, 1, pp.157–160.
5. Raju, K., et al., 2023. Insights into the potent anticancer activity of Couroupita guianensis Aubl.—a review. Pakistan Heart Journal, 56, pp.1136–1139.
6. H., H., et al., 2022. Screening of phytochemicals from Couroupita guianensis as drug candidates against lethal diseases using in silico analysis. International Journal of Applied Chemistry and Biological Sciences, 3, pp.9–19.
7. Shantilal, S., Vaghela, J.S., Sisodia, S., 2018. Review on immunomodulation and immunomodulatory activity of some medicinal plant. European Journal of Biomedical, 5, pp.163–174.
8. Sheba, L.A., Anuradha, V., 2019. An updated review on Couroupita guianensis Aubl: A sacred plant of India with myriad medicinal properties. Journal of Herbmed Pharmacology, 9, pp.1–11.
9. Teixeira, N., et al., 2019. Edible fruits from Brazilian biodiversity: A review on their sensorial characteristics versus bioactivity as tool to select research. Food Research International, 119, pp.325–348.
10. Sundararajan, R., Koduru, R., 2014. A complete profile on Couroupita guianensis: Traditional uses, pharmacological activities and phytoconstituents. Pharmacophore, 5, pp.147–159.
11. Bafna, A., Mishra, S., 2010. Antioxidant and immunomodulatory activity of the alkaloidal fraction of Cissampelos pareira Linn. Scientia Pharmaceutica, 78, pp.21–32.
12. Jagannatha, S., Maity, S., Santra, A., Kuruvalli, G., Reddy, V.D., Golla, R., 2025. An updated review on ethnomedicinal uses, phytochemistry and pharmacological activities of Couroupita guianensis. Pharmacognosy Reviews, 18(36), pp.111–116. https://doi.org/10.5530/phrev.20241935
13. Augusco, M.A.C., Sarri, D.A., Panontin, J.F., Rodrigues, M.A.M., Fernandes, R.M.N., Silva, J.F.M.D.,

Cardoso, C.A.L., Rambo, M.K., Scapin, E., 2023. Extracts from the leaf of Couroupita guianensis (Aubl.): Phytochemical, toxicological analysis and evaluation of antioxidant and antimicrobial activities against oral microorganisms. Plants, 12, 2327.

14. Tena, N., Asuero, A.G., 2022. Up-to-date analysis of the extraction methods for anthocyanins: Principles of the techniques, optimization, technical progress, and industrial application. Antioxidants, 11, 286.
15. Dubale, S., Kebebe, D., Zeynudin, A., Abdissa, N., Suleman, S., 2023. Phytochemical screening and antimicrobial activity evaluation of selected medicinal plants in Ethiopia. Journal of Experimental Pharmacology, 15, pp.51–62.
16. Gomathi, D., Kalaiselvi, M., Ravikumar, G., Devaki, K., Uma, C., 2015. GC-MS analysis of bioactive compounds from the whole plant ethanolic extract of Evolvulus alsinoides (L.) L. Journal of Food Science and Technology, 52, pp.1212–1217.
17. Kuruvalli, G., Lavanya, L., Pulakuntla, S., Prashantha, C.N., Shaik, A.H., Reddyvari, H., Reddy, V.D., 2024. Vitex negundo L. leaf extract suppresses the cell cycle and promotes apoptosis in colon cancer cells. Indian Journal of Biochemistry and Biophysics, 61, pp.269–278.
18. Hussen, E.M., Endalew, S.A., 2023. In vitro antioxidant and free-radical scavenging activities of polar leaf extracts of Vernonia amygdalina. BMC Complementary Medicine and Therapies, 23, 146.
19. Da, X., Nishiyama, Y., Tie, D., et al., 2019. Antifungal activity and mechanism of action of Ou-gon (Scutellaria root extract) components against pathogenic fungi. Scientific Reports, 9, 1683.
20. Gouthami, K., Veeraraghavan, V., Lavanya, L., Prashantha, C.N., 2022. Molecular docking studies for Vitex negundo (L.) leaf extract compounds against Wnt-signalling proteins towards the treatment of colon cancer. Chemistry of Data Collections, 38, 100829.
21. Prabhakaran, P., Hebbani, A.V., Menon, S.V., et al., 2023. In silico generation of novel ligands for the inhibition of SARS-CoV-2 main protease (3CLpro) using deep learning. Frontiers in Microbiology, 14, 1194794.
22. Gu, Y., Yu, Z., Wang, Y., et al., 2024. admetSAR3.0: A comprehensive platform for exploration, prediction and optimization of chemical ADMET properties. Nucleic Acids Research, 52, pp.W432–W438.
23. Kumari, D., Vhanmane, V.R., Gouthami, K., Reddy, V.D., Nagendra, G., 2024. 2-DPC mediated effective synthesis of peptide conjugates, their antifungal and antibacterial properties. Chemistry Select, 9, e202402123.
24. Gouthami, K., Veeraraghavan, V., Nagaraja, P., 2022. In-silico characterization of phytochemicals identified from Vitex negundo (L.) extract as potential therapy for Wnt-signaling proteins. Egyptian Journal of Medical Human Genetics, 23, pp.1–15.
25. Pulakuntla, S., Singh, S.A., Kuruvalli, G., Shaik, A.H., Reddy, V.D., 2024. Molecular docking and dynamics analysis to reveal the therapeutic potential of dostarlimab against novel immune targets in liver cancer. Indian Journal of Biochemistry and Biophysics, 61, pp.740–755.
26. Hayat, J., Akodad, M., Moumen, A., et al., 2020. Phytochemical screening, polyphenols, flavonoids and tannin content, antioxidant activities and FTIR characterization of Marrubium vulgare L. from two different localities of northeast of Morocco. Heliyon, 6, e05609.
27. Munteanu, G., Apetrei, C., 2021. Analytical methods used in determining antioxidant activity: A review. International Journal of Molecular Sciences, 22, 3380.
28. Gizaw, A., Marami, L.M., Teshome, I., et al., 2022. Phytochemical screening and in vitro antifungal activity of selected medicinal plants against Candida albicans and Aspergillus niger in West Shewa zone, Ethiopia. Advances in Pharmacological and Pharmaceutical Sciences, 2022, 3299146.
29. Lipinski, A.A., 2004. Lead-and drug-like compounds: The rule-of-five revolution. Drug Discovery Today: Technologies, 1, pp.337–341.
30. Srivastava, R., 2021. Theoretical studies on the molecular properties, toxicity, and biological efficacy of 21 new chemical entities. ACS Omega, 6, pp.24891–24901.
31. Dulsat, B., López-Nieto, B., Estrada-Tejedor, R., Borrell, J.I., 2023. Evaluation of free online ADMET tools for academic or small biotech environments. Molecules, 28, 776.
32. Altemimi, A., Lakhssassi, N., Baharlouei, A., Watson, D.G., Lightfoot, D.A., 2017. Phytochemicals: Extraction, isolation, and identification of bioactive compounds from plant extracts. Plants, 6, 42.

33. Cosconati, S., Forli, S., Perryman, A.L., et al., 2010. Virtual screening with AutoDock: Theory and practice. Expert Opinion on Drug Discovery, 5, pp.597–607.
34. Ghahremanian, S., Rashidi, M.M., Raeisi, K., Toghraie, D., 2022. Molecular dynamics simulation approach for discovering potential inhibitors against SARS-CoV-2: A structural review. Journal of Molecular Liquids, 354, 118901.
35. Gheidari, D., Mehrdad, M., Karimelahi, Z., 2024. Virtual screening, ADMET prediction, molecular docking, and dynamic simulation studies of natural products as BACE1 inhibitors for the management of Alzheimer's disease. Scientific Reports, 14, 26431.